frontiers | Frontiers in Environmental Science

ORIGINAL RESEARCH
published: 04 May 2022
doi: 10.3389/fenvs.2022.888252

Characterization of Montmorillonite–Biochar Composite and Its Application in the Removal of Atrazine in Aqueous Solution and Soil

*Pingping Wang[1], Marianne Stenrød[2], Liang Wang[3], Shankui Yuan[4], Liangang Mao[1], Lizhen Zhu[1], Lan Zhang[1], Yanning Zhang[1], Hongyun Jiang[1], Yongquan Zheng[1] and Xingang Liu[1]**

[1]State Key Laboratory for Biology of Plant Disease and Insect Pests, Institute of Plant Protection, Chinese Academy of Agricultural Sciences, Beijing, China, [2]Norwegian Institute of Bioeconomy Research (NIBIO), Høgskoleveien, Norway, [3]SINTEF Energy Research, Trondheim, Norway, [4]Environment Division, Institute for the Control of Agrochemicals, Ministry of Agriculture and Rural Affairs, Beijing, China

Atrazine is a widely used triazine herbicide, which poses a serious threat to human health and aquatic ecosystem. A montmorillonite–biochar composite (MMT/BC) was prepared for atrazine remediation. Biochar samples were characterized by using scanning electron microscope (SEM), transmission electron microscopy (TEM), Fourier transform infrared spectroscopy (FTIR), and X-ray photoelectron spectrometer (XPS). Structural and morphological analysis of raw biochar (BC) and MMT/BC showed that MMT particles have been successfully coated on the surface of biochar. Sorption experiments in aqueous solution indicated that the MMT/BC has higher removal capacity of atrazine compared to BC (about 3.2 times). The sorption of atrazine on the MMT/BC was primarily controlled by both physisorption and chemisorption mechanisms. The amendment of MMT/BC increased the sorption capacity of soils and delayed the degradation of atrazine. Findings from this work indicate that the MMT/BC composite can effectively improve the sorption capacity of atrazine in aquatic environment and farmland soil and reduce the environmental risk.

Keywords: montmorillonite–biochar composite, atrazine, sorption, degradation, soil

OPEN ACCESS

Edited by:
Oladele Ogunseitan, University of California, Irvine, United States

Reviewed by:
Kassio Ferreira Mendes, Federal University of Viçosa, Brazil
Huacheng Xu, Nanjing Institute of Geography and Limnology (CAS), China

****Correspondence:***
Xingang Liu
liuxingang@caas.cn

Specialty section:
This article was submitted to Toxicology, Pollution and the Environment, a section of the journal Frontiers in Environmental Science

Received: *02 March 2022*
Accepted: *08 April 2022*
Published: *04 May 2022*

Citation:
Wang P, Stenrød M, Wang L, Yuan S, Mao L, Zhu L, Zhang L, Zhang Y, Jiang H, Zheng Y and Liu X (2022) Characterization of Montmorillonite–Biochar Composite and Its Application in the Removal of Atrazine in Aqueous Solution and Soil. Front. Environ. Sci. 10:888252. doi: 10.3389/fenvs.2022.888252

INTRODUCTION

Atrazine, 6-chloro-N2-ethyl-N4-isopropyl-1,3,5-triazine-2,4-diamine, is a widely used triazine herbicide used for controlling annual grasses and broadleaf weeds (Solomon et al., 1996). Due to its persistence, moderate aqueous solubility (35 mg/L), high mobility, and long half-life, atrazine has a high detection rate in surface water, groundwater, and soil (Tappe et al., 2002; Qu et al., 2017; Zheng et al., 2019). In the Hubei Province of central China, atrazine was detected in the sediments of six eutrophic lakes, and the highest concentration of atrazine was found to be 0.171 mg/kg in Honghu Lake (Qu et al., 2017). Atrazine was also detected in two soils in Belgium and Germany (8.3 and 15.2 μg/kg, respectively), even in soils not treated with atrazine (Jablonowski et al., 2010). In addition, atrazine has been categorized as an endocrine disruptor and a probable human carcinogen, which may affect the central nervous system and immune systems and even affect human semen quality and fertility (Hayes et al., 2003; Swan et al., 2003; Chen et al., 2009). Atrazine has been banned

in some European countries, but it is still widely used in China. Therefore, it is necessary to develop a reliable and effective treatment to remove or sequester atrazine from aquatic environment and farmland soil to reduce the environmental and health risk of atrazine.

Biochar, a carbon-rich solid material, is produced by pyrolysis of biomass with limited or without oxygen (Novak et al., 2009). As an excellent remediation agent, biochar has been widely used in wastewater and soil to immobilize or sequester pesticides, such as herbicides and insecticides, through sorption, partition, and pore diffusion (Zheng et al., 2010; Yu et al., 2011; Li et al., 2018). Liu et al. (2015) reported that soybean biochar has much higher atrazine removal ability in aqueous solution. Jin et al. (2016) indicated that biochar would be helpful to stabilize soil contaminated with imidacloprid, isoproturon, and atrazine. Our previous research found that peanut shell biochar also had a good sorption effect on atrazine (Wang et al., 2020). Therefore, biochar can effectively reduce the environmental risk of atrazine. Many studies have shown that the degradation degree of pesticides in soil is different after adding biochar. Generally, biochar-amended soil increases sorption of pesticides and reduces bioavailability of soil to microorganisms, which reduces the biodegradation of pesticides and prolongs the half-life of pesticides (Yang et al., 2010; Yu et al., 2011; Li et al., 2017b). However, some studies have found that the organic matter of biochar can enhance the biological activity of microorganisms by providing nutrients so as to accelerate the degradation of pesticides (Fang et al., 2016; Wu et al., 2019). Singh et al. (2022) found that the addition of biochar to the soils increased the half-life of atrazine and significantly improved the recovery process of soil biological activities under atrazine stress.

Recently, the combination of biochar and clay has been widely used for pollutant removal in order to improve the structure and sorption characteristics of biochar (Zhang and Gao, 2013; Yao et al., 2014; Tang et al., 2015). Clay minerals are abundant natural resources with inexpensive, high surface area, cation exchange capacity, and structural properties. Montmorillonite (MMT) is the most commonly studied clay material, which is an irregular lamellar crystal composed of layers of one octahedral and two tetrahedral sheets (Zhu et al., 2019). The fine particles of MMT are unsuitable for water treatment, but in a composite form, biochar has a good porous structure to support MMT (Chen et al., 2017). In addition, MMT could provide exogenous metal atoms (i.e., aluminum and magnesium), which may be embedded to react with biochar, forming a high-performance biochar complex (Song et al., 2020). The composite makes full use of the good sorption capacity of biochar and MMT to become a low-cost and effective sorbent. However, research on the effect of MMT/BC on sorption and degradation of contaminants, as well as on the removal of contamination from aqueous solution and soil, was scarce.

Therefore, the aims of this study were to (1) develop a low-cost and effective MMT–biochar composite by using a simple and low-cost method, (2) assess the ability and mechanisms of atrazine removal from aqueous solutions, and (3) evaluate the effects of MMT–biochar composite on the sorption and degradation of atrazine in different soil. This study provides useful information for better evaluation of the potential of biochar–clay composite in reducing pesticide residues.

MATERIALS AND METHODS

Reagents and Chemicals

Standard atrazine (purity 99.2%) was obtained from Shenyang Research Institute of Chemical Industry (Shenyang, China). HPLC-grade acetonitrile, formic acid, and sodium azide (NaN_3) were purchased from Sigma-Aldrich (Steinheim, Germany). All analytical reagents including calcium chloride ($CaCl_2$), sodium chloride (NaCl), anhydrous magnesium sulfate ($MgSO_4$), sodium hydroxide (NaOH), and hydrochloric acid (HCl) were obtained from Sinopharm Chemical Reagent Co., Ltd (Beijing, China). MMT was purchased from Shanghai Macklin Biochemical Co., Ltd (Shanghai, China). Ultrapure water was prepared using a Milli-Q reagent water system (Bedford, MA, United States).

Biochar and Soil Preparation and Characterization

Peanut shells were collected from the Shandong Province of China, washed with tap water to remove the surface dust and soil, dried at 70°C, and then crushed by using a high-speed pulverizer and passed through an 18-mesh sieve. A stable MMT suspension was prepared by adding MMT powder to 100 ml ultrapure water and mixed with ultrasound for 30 min. Then, 20 g peanut shells were immersed in MMT suspensions, stirred by magnetic stirrer for 2 h, and dried in oven at 105°C for 12 h. The impregnated samples were placed in a quartz boat of a tubular furnace (Zhonghuan Experimental Furnace Co., Ltd., Tianjin, China), pyrolyzed in a continuous flow of N_2, heated at a rate of 5°C/min, and maintained for 1 h when the pyrolysis temperature reached 600°C. The produced biochar samples were crushed, passed through an 80-mesh sieve, stored in a brown ground glass bottle, and sealed in a dryer. In total, five types of MMT–biochar composites were prepared by changing the mass ratio of MMT to BC (i.e., 20, 25, 30, 40, and 50%), and the resulting products were designated as 20% MMT/BC, 25% MMT/BC, 30% MMT/BC, 40% MMT/BC, and 50% MMT/BC, respectively. At the same time, peanut shells were treated with the same method to prepare BC as control. Unless otherwise specified, the MMT/BC mentioned later is 25% MMT/BC. By changing the pyrolysis temperature, MMT/BC under different temperature conditions was prepared, and the pyrolysis temperature was set to 400, 500, and 600 °C, respectively.

Elemental analysis using surface structure, scanning electron microscope (SEM), Fourier transform infrared spectroscopy (FTIR), and X-ray photoelectron spectrometer (XPS) was based on our previous analysis methods (Wang et al., 2020). Transmission electron microscopy (TEM) (FEI, Thermo Fisher Scientific, United States) was used to observe the microstructure of the biochar. Zeta potential of biochar was determined using a Zetasizer Nano ZS90 (Malvern Instruments, Malvern,

United Kingdom). The pH value of the solution was measured by using a pH meter (FiveEasy Plus, Mettler Toledo, United States).

Two kinds of agricultural soil without detectable atrazine were collected from Jilin (44°23′52″N, 125°10′2″E) and Shandong provinces (36°12′43″N, 116°41′29″E) of China, denoted as S-DB and S-SD, respectively. The soils were taken at the top 10 cm and screened by using a 2 mm sieve for sorption and degradation experiments. The physicochemical properties of the S-DB showed it to be sandy loam (65.4% sand, 15.1% silt, and 19.5% clay) with pH 7.83, 41.0 g/kg organic matter, 1.15% organic carbon, and 17.2 cmol (+)/kg CEC. The S-SD also belonged to sandy loam (57.9% sand, 17.3% silt, and 24.8% clay) with pH 7.24, 29.2 g/kg organic matter, 0.39% organic carbon, and 21.4 cmol (+)/kg cation exchange capacity (CEC).

Sorption Experiments of Biochar in Aqueous Solution

To determine the effect of MMT dosage (0, 20, 25, 30, 40, and 50%) and pyrolysis temperature (400, 500, and 600°C) on the removal of atrazine, 100 mg biochar and 40 ml of 10 mg/L atrazine aqueous solution (contained 0.01 mol/L $CaCl_2$ and 200 mg/L NaN_3) were introduced into 50 ml brown sample bottles. The bottles were then sealed and shaken in the dark on a reciprocating shaker at 180 rpm and 25 ± 1°C for 72 h. The pH of the mixtures was adjusted to 7.0 ± 0.2 using 0.1 M HCl/NaOH and monitored during and after sorption. The same conditions were used to test the effects of initial pH in the range of 2–9 on MMT/BC sorption. After the experiments, the bottles were put to rest for 10 min to make the biochar samples sink into the bottom by gravity to achieve solid–liquid separation, and the supernatant was filtered using a 0.22 μm membrane filter. The filtered solutions were then stored at −20°C until analysis.

The sorption kinetic and isotherm of atrazine were carried out on BC and MMT/BC using the same conditions and procedures, as described before. The kinetic tests were conducted with an initial atrazine concentration of 10 mg/L, 150 mg of BC, or 50 mg of MMT/BC per 40 ml atrazine solution. Duplicate bottles were sampled at predetermined times (1, 2, 4, 6, 8, 10, 12, 24, 48, and 72 h) and analyzed for atrazine concentration in the solution. In the sorption isotherm experiment, 150 mg BC or 50 mg MMT/BC was mixed with 40 ml atrazine solution with the concentration of 0.25–30 mg/L for 72 h.

Under the same conditions, the solutions without biochar were set for the control test. The loss of atrazine was negligible, including hydrolysis and sorption on the bottle wall. Based on the initial and final concentration of atrazine in solution and the dosage of biochar, the sorption capacity of atrazine on biochar was calculated.

Sorption Experiments on Soil and Biochar–Soil Mixtures

The sorption isotherms of atrazine on biochar and biochar–soil mixtures were determined by three repeated batch sorption experiments under eight initial concentrations of atrazine (0.25–30 mg/L). A 5 g aliquot of soil with or without 50 mg BC or MMT/BC was weighed into a 50 ml centrifuge tube. Then, 25 ml of the background solution containing 0.01 M $CaCl_2$ and 200 mg/L NaN_3 was added. According to the initial concentration, a certain amount of atrazine stock solution was added to the centrifuge tube, the cover was tightened, and then shaken for 72 h at 180 rpm and 25 ± 1°C in the dark. At the end of the experiment, the tubes were centrifuged at 4,000 rpm for 10 min, and 1.5 ml of supernatant was filtered into the injection vial through 0.22 μm membrane filter. The filtered solutions were stored at −20°C until analysis.

Degradation Experiments

Before the degradation experiments, a part of the collected soil was pre-cultured with a moisture content of 60% of the water holding capacity in the dark incubator (25 ± 1°C) for 2 weeks, and the other part was sterilized at 121°C for 30 min in an autoclave (Lead-Tech Scientific Instruments Co., Ltd, Shanghai, China). MMT/BC was chosen to investigate the impacts on atrazine degradation in the two soils. First, an aliquot of 20 g soil (dry weight) or the biochar–soil mixture (4 g of MMT/BC) was weighed into a 500 ml glass bottle, and then 100 μL of the atrazine acetone stock solution (10,000 mg/L) was added into the bottle. The soil samples were kept for 10 min until the acetone volatilized completely and then vortexed for 5 min. Next, another 180 g soil was weighed into the bottle, vortexed for 30 min, and mixed well with the spiked soil; the final concentration of atrazine in soil was 5 mg/kg (dry weight). After that, 15 g of spiked soil was weighted into 50 ml pre-cleaned glass bottle, and the soil moisture content was adjusted with ultrapure water to 60% of the saturated soil moisture content. In the same operation, the sterilized ultrapure water containing 200 mg/L NaN_3 was added into the sterilized soil to inhibit the growth of microorganisms. The bottles were stoppered with cotton and cultured in the dark in an incubator under constant temperature (25 ± 1°C) and humidity (70%). The water content was monitored regularly during soil incubation to maintain the initial state of soil moisture. Triplicate sample bottles of each treatment were removed after predetermined incubation times (0, 1, 3, 5, 7, 14, 21, 30, 40, 60, 90, and 120 days), and the soil samples were freeze-dried and stored at −20°C until extraction. Details of the soil sample treatment are shown in **Supplementary Text S1**.

Data Analysis

Different mathematical models including first-order, second-order, and Elovich models were used to fit the kinetics data (Inyang et al., 2014; Yao et al., 2014; Liu et al., 2015):

$$\text{First} - \text{order}: \ q_t = q_e\left(1 - e^{-k_1 t}\right), \tag{1}$$

$$\text{Second} - \text{order}: \ q_t = \frac{k_2 q_e^2 t}{1 + k_2 q_e^2 t}, \tag{2}$$

$$\text{Elovich}: \ q_t = \frac{1}{\beta}\ln(\alpha\beta t + 1), \tag{3}$$

TABLE 1 | Physical and chemical characteristics of BC and MMT/BC.

Biochar	Elemental composition (%)				Atomic ratio			SA[a] (m^2/g)	PV[b] (cm^3/g)	PD[c] (nm)
	C	H	N	O	H/C	O/C	(O + N)/C			
BC	87.35	3.61	0.81	6.53	0.50	0.06	0.06	262.86	0.014	4.4438
MMT/BC	50.91	2.61	0.50	6.33	0.62	0.09	0.10	233.16	0.066	12.0242

[a]*SA, surface area determined by the BET adsorption method.*
[b]*PV, pore volume.*
[c]*PD, pore diameter.*

where q_t and q_e represent the amount of atrazine removed at time t and at equilibrium, respectively (mg/kg); k_1 and k_2 are the sorption rate constants (1/h); α represents the initial sorption rate (mg/kg); and β represents the desorption constant (kg/mg).

Three models (Freundlich, Langmuir, and dual-mode) were used to fit the isotherm experimental data (Uchimiya et al., 2010; Zhang et al., 2011; Suo et al., 2019):

$$\text{Freundlich}: \ q_e = K_f C_e^n, \tag{4}$$

$$\text{Langmuir}: \ q_e = \frac{q_m K C_e}{1 + K C_e}, \tag{5}$$

$$\text{Dual} - \text{mode}: \ q_e = \frac{bQC_e}{1 + bC_e} + K_D C_e, \tag{6}$$

where q_e represents the atrazine concentration on the solid-phase at equilibrium (mg/kg), C_e represents the solution concentration of atrazine at equilibrium (mg/L), K_f [(mg/kg)/(mg/L)^n] and K (L/mg) represent affinity coefficient, n represents the Freundlich linearity constant, b represents the affinity constant (L/mg), K_D represents the partition domain coefficient (L/kg), and q_m and Q represents the maximum capacity (mg/kg).

The first-order reaction kinetic model was used to fit the data of atrazine degradation kinetics in soil and biochar–soil mixtures (Zhang et al., 2018):

$$C_t = C_0 e^{-kt}, \tag{7}$$

where C_0 is the initial concentration of atrazine (mg/kg), C_t is the concentration of atrazine (mg/kg) at sampling time t (d), k is the degradation rate constant (d^{-1}), and the half-life ($t_{1/2}$) was ln2/k.

The experimental data were fitted by Origin 9.1. The statistical analyses were analyzed by SPSS 25.0 one-way analysis of variance (ANOVA).

RESULTS AND DISCUSSION

Characterization of Biochar

The properties of biochar varied greatly between BC and MMT/BC. The elemental composition (C, N, H, and O) of BC and MMT/BC, presented in **Table 1**, suggested that the addition of MMT reduced the content of C, N, H, and O, especially the carbon content, from 87.35% to 50.91%. The surface area of MMT/BC was slightly decreased from 262.86 to 233.16 m^2/g, which may be related to the pore coating or plugging caused by the existence of MMT minerals (Yao et al., 2014). The total pore volume and the average pore diameter of the MMT/BC were increased from 0.014 to 0.066 cm^3/g and 4.44–12.02 nm in comparison with BC. This is probably because MMT is layered silicate mineral, which contains mineral elements with small surface areas and abundant transitional pores (Li et al., 2015; Li et al., 2017a; Yao et al., 2014). The N_2 adsorption–desorption isotherms and pore size distribution of MMT/BC and BC are shown in **Supplementary Figure S1**. As described by the International Union of Pure and Applied Chemistry (IUPAC), the isotherms of BC evolved to type I, which shows the characteristic of a microporous material (Jing et al., 2014). The N_2 isotherms of MMT/BC resemble those of type II, and the observed hysteresis curves of MMT/BC is of type H4, indicating the narrow cracks and pores in the sorbent materials (Jing et al., 2014). In the pore size distribution curve (**Supplementary Figure S1B**), BC and MMT/BC exhibited heterogenous pore structures, and mesopore (2–50 nm) was the main pore structure.

The SEM images of BC and MMT/BC are shown in **Figures 1A,B**. Surface and pore filling mechanisms may be responsible for the removal of atrazine as the pores were observed on biochar surfaces. The SEM images of MMT/BC clearly showed that MMT particles adhered to the biochar surface and completely coated the pure biochar, changing the surface morphologies and providing more sorption sites (Liang et al., 2019; Premarathna et al., 2019). Also, the MMT did not block the pores of biochar, which ensures the accessible to the adsorbate molecules (Premarathna et al., 2019). TEM imaging of the MMT/BC (**Figure 1D**) showed that the biochar surface was widely covered by the layered structures compared with BC (**Figure 1C**). In addition, it is reported that the structure is a common clay structural morphology (Tyagi et al., 2006; Zhou et al., 2009).

As shown in FTIR (**Figure 2**), the spectrum at ~3,400 cm^{-1} showed stretching vibrations of O-H, ~1,580 cm^{-1} was related to stretching vibration of C=C of the aromatic ring (Chen et al., 2008; Keiluweit et al., 2010). The band observed around 1,050 cm^{-1} was related to the Si-O functional groups on the MMT/BC surface (Tyagi et al., 2006; Chen et al., 2017). The bands appearing below 800 cm^{-1} of MMT/BC could be attributed to Si-O stretching, Si-O-Mg bending, Si-O-Al bending, and Si-O-Si bending (Zhou et al., 2009; Chen et al., 2017).

Raman spectra (**Supplementary Figure S2**) showed two prominent peaks at ~1,350 cm^{-1} and ~1,600 cm^{-1}, representing D-band originated from sp^3 hybridization with disordered mode and G-band induced by crystalline

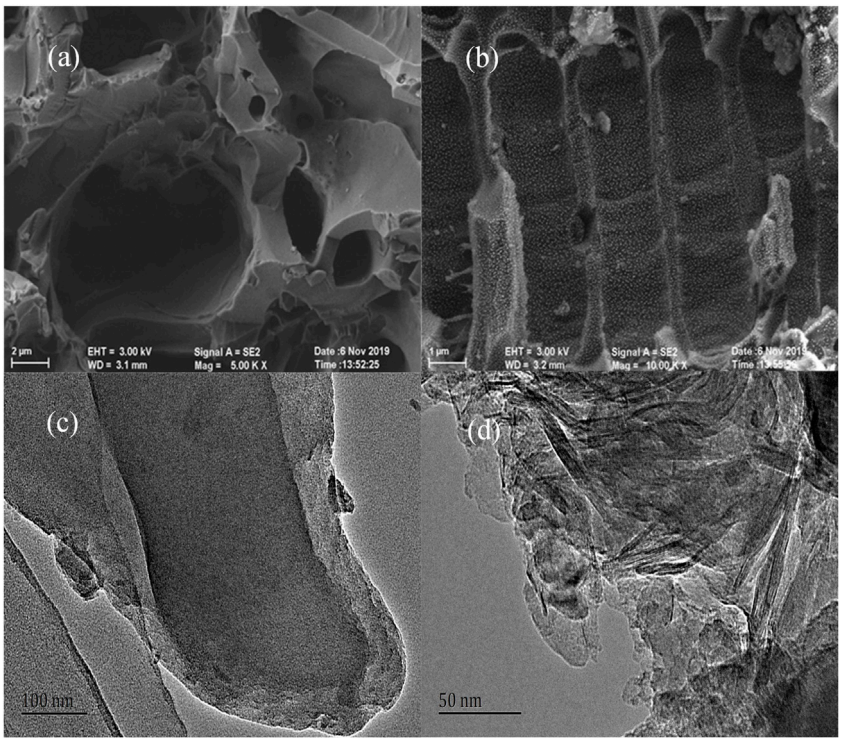

FIGURE 1 | SEM images of BC **(A)** and MMT/BC **(B)**; TEM images of BC **(C)** and MMT/BC **(D)**.

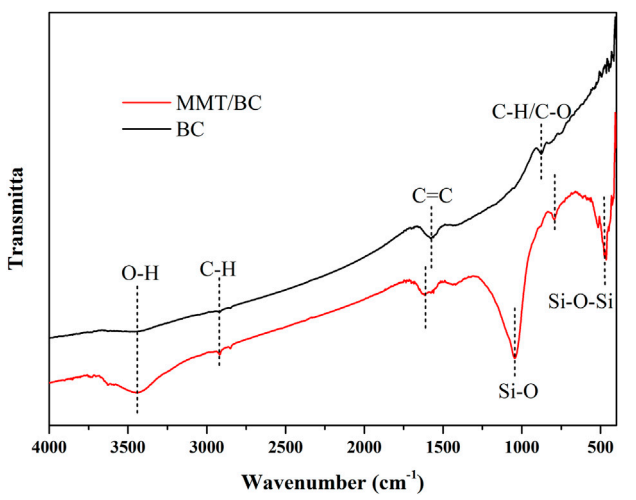

FIGURE 2 | FTIR spectra of BC and MMT/BC.

graphitic/sp^2 carbon stretching vibrations with the tangential mode, respectively (Ferrari and Robertson, 2000; Akhavan, 2010). The higher ratio of I_D/I_G peak intensity means higher defect concentration and increased functional groups on the sorbents surface. The I_D/I_G decrease from 1.04 for BC to 1.00 for MMT/BC, which was not a significant change.

Zeta potentials of MMT/BC are depicted in **Supplementary Figure S3**. In the pH range between 2 and 9, the MMT/BC resulted in a zeta potential drop of 35 mV. The MMT/BC surface was negatively charged at pH values greater than the point of zero charge pH (pH_{pzc}, 2.7) and was positively charged at pH values lower than pH_{pzc} (Nandi et al., 2009).

The full XPS spectra representing the chemical composition and crystalline states are displayed in **Figures 3A,E**. For MMT/BC, the six peaks at 285.0, 400.0, 532.6, 74.0, 103.2, and 1,304.3 eV were attributed to the element of C, N, O, Al, Si, and Mg on the surface, respectively, while there are no obvious peaks corresponds to Al, Si, and Mg on the surface of BC. The high-resolution C 1s spectra (**Figures 3B,F**) could be deconvoluted into four peaks: C-C/C-H (~284.8 eV), C-O (~286.4 eV), C=O (~288.0 eV), and O-C=O (~289.5 eV) (Gao et al., 2018; Liu et al., 2015). The O 1s spectra (**Figures 3C,G**) could be attributed into three groups: C=O (~531.6 eV), -OH (~532.5 eV), and C-O (~534.1 eV) (Lyu et al., 2017b; Zhou et al., 2007). The N 1s spectra of BC (**Figure 3D**) can be deconvoluted into two peaks at 398.7 and 400.6 eV, which can be assigned to the pyridinic N (C-N=C) and pyrrolic N (C-N). A new peak corresponding to graphitic N can be found at 402.0 eV for MMT/BC (**Figure 3H**) (Jansen and Van Bekkum, 1995; Lyu et al., 2017a; Mueller et al., 2015). **Supplementary Table S1** listed their relative percentages on BC and MMT/BC. For C 1s, the C-O ratio of biochar increased from 8.74% to 12.09% after MMT was added, and the C=O ratio increased from 4.52% to 4.98%, indicating the participation of oxygen-containing functional groups (Liang et al., 2019). For O

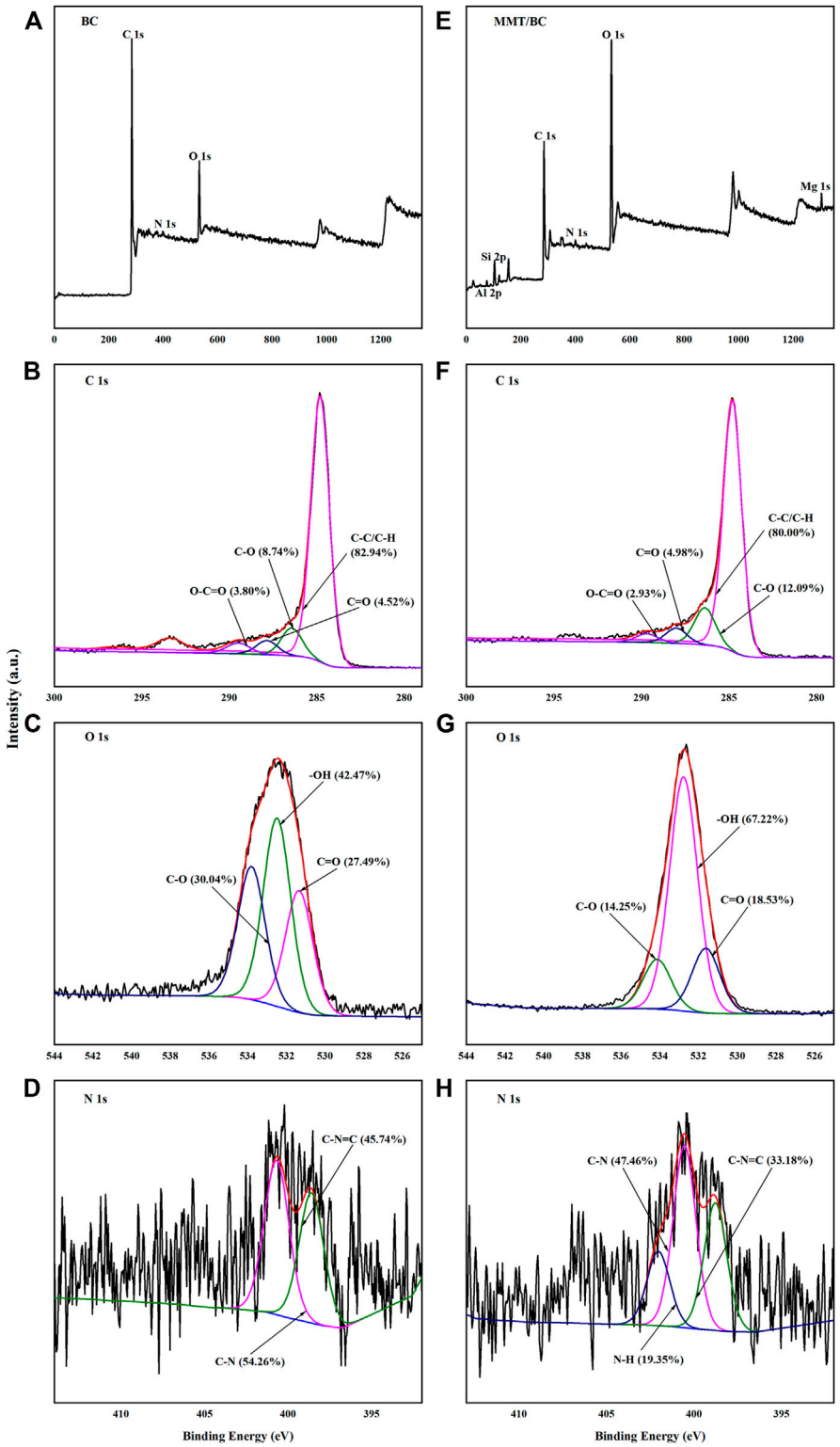

FIGURE 3 | XPS spectra of BC **(A–D)** and MMT/BC **(E–H)**. **(A,E)** Wide survey scan, **(B,F)** C 1s, **(C,G)** O 1s, **(D,H)** N 1s.

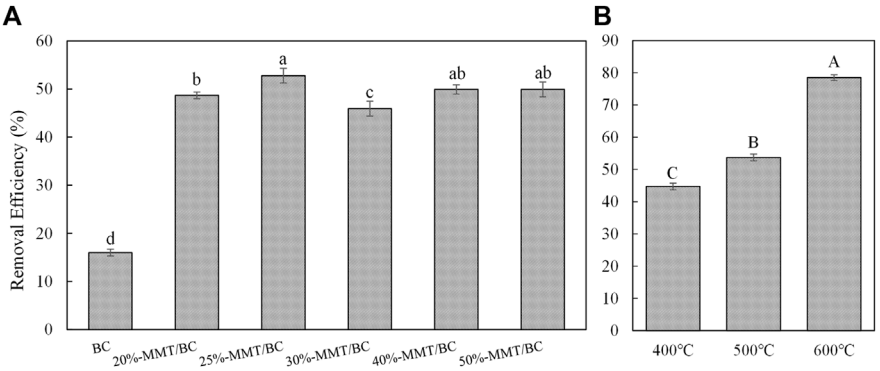

FIGURE 4 | Effects of MMT dosage during biochar preparation **(A)** and pyrolysis temperature of MMT/BC **(B)** on atrazine removal efficiency. Values with lowercase letters are different from each other ($p < 0.05$), and values with capital letters are significantly different from each other ($p < 0.01$).

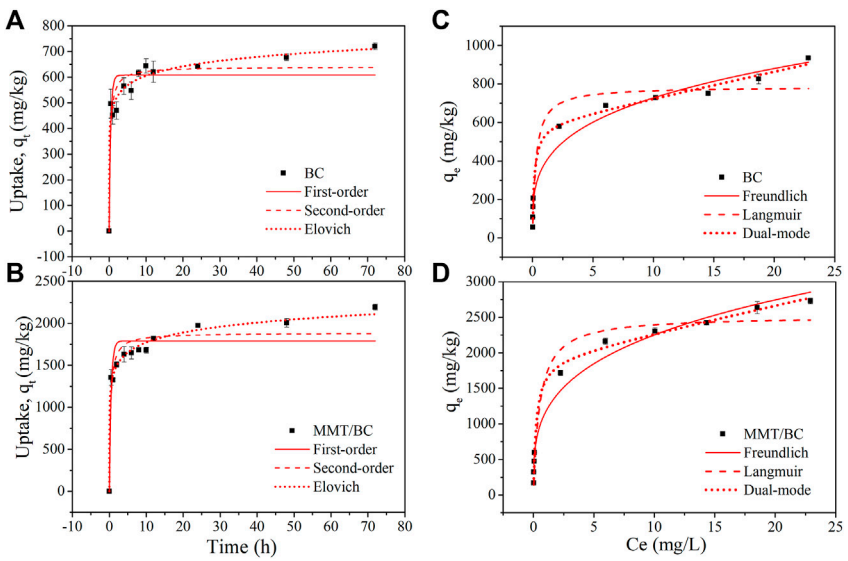

FIGURE 5 | Sorption kinetics **(A,B)** and sorption isotherms **(C,D)** of atrazine on BC and MMT/BC. Kinetic data were fitted to first-order, second-order, and Elovich models. Isotherm data were fitted to Freundlich, Langmuir, and dual-mode models. Error bars indicate SD.

1s, the -OH ratio of biochar increased from 42.47% to 67.22% after MMT was added, and the effect of MMT/BC on atrazine had hydrogen bond involvement.

Sorption of Atrazine on Biochar

Effects of MMT Dosage

The effects of MMT rate during biochar preparation on the removal efficiency of atrazine were investigated. As shown in **Figure 4A**, the removal efficiency of atrazine significantly ($p < 0.05$) increased from 16.01% (BC) to 52.78% (25% MMT/BC) with an increase of the MMT contents from 0 to 25%, suggesting a 36.77% increase. However, relatively lower removal efficiencies were obtained by other dosage (20, 30, 40, and 50%), suggesting 29.89%–33.90% increase compared to the control (BC). The surface of BC coated with MMT led to its larger pore size and volume (**Table 1**), especially the reactive surface area and CEC (Yao et al., 2014; Chen et al., 2017); therefore, the combination of MMT and biochar is particularly effective in the removal of atrazine. However, the excessive clay particles could block the pores of biochar, resulting in the decrease of available sorption sites and sorption capacity of the composite (Yao et al., 2014; Fosso-Kankeu et al., 2015). Therefore, 25% MMT was the best ratio of composite materials, and 25% MMT/BC was selected for sorption experiment and identification of sorption mechanism in aqueous solution, as well as sorption and degradation experiments in soils.

Effects of Pyrolysis Temperature

As shown in **Figure 4B**, with the increase of pyrolysis temperature, the removal efficiency of atrazine by

TABLE 2 | Fitting parameters of sorption kinetics and sorption isotherms of atrazine on BC and MMT/BC.

Sorption kinetics	Biochar	First-order			Second-order			Elovich		
		qe (mg/kg)	k1 (1/h)	R2	qe (mg/kg)	k2 (1/h)	R2	α (mg/kg)	β (kg/mg)	R2
	BC	608 ± 26	2.34 ± 0.74	0.836	641 ± 23	(5.34 ± 1.93) × 10–3	0.909	(4.71 ± 5.64) × 105	0.019 ± 0.0022	0.974
	MMT/BC	1791 ± 73	2.02 ± 0.57	0.848	1887 ± 67	(1.61 ± 0.54) × 10–3	0.914	(5.47 ± 3.61) × 105	(5.85 ± 0.42) × 10–3	0.988

Sorption isotherms	Biochar	Freundlich			Langmuir			Dual-mode			
		Kf (mg/kg)/(mg/L)n	n	R2	qm (mg/kg)	K (L/mg)	R2	b (L/mg)	Q (mg/kg)	KD (L/kg)	R2
	BC	386 ± 28	0.28 ± 0.028	0.967	786 ± 38	3.55 ± 1.49	0.940	6.46 ± 1.08	593 ± 29	13.76 ± 1.89	0.992
	MMT/BC	1,164 ± 80	0.29 ± 0.026	0.974	2,518 ± 111	1.93 ± 0.74	0.961	4.37 ± 0.55	1920 ± 66	38.20 ± 4.28	0.996

± represents the SE of the fitting parameter.

MMT–biochar composites increased from 44.72% (400°C) to 53.71% (500°C) and 78.50% (600°C). Our previous study (Wang et al., 2020) found that in the low concentration (about <15 mg/L) the sorption capacity of peanut shell biochar for atrazine increased with the increase of pyrolysis temperature. The results showed that biochar composites are also affected by pyrolysis temperature, 600°C was taken as the pyrolysis temperature of MMT/BC. This temperature was also used to prepare clay–biochar composite materials by Yao et al. (2014).

Sorption Kinetics of Atrazine on Biochar

Sorption kinetics of atrazine on BC and MMT/BC are shown in **Figures 5A,B**. The kinetics experiment data showed that the uptake of atrazine by BC and MMT/BC increased rapidly from 0 to 496.00 and 1,353.49 mg/kg in the first half hour, respectively, and increased steadily after 12 h (620.75 mg/kg for BC and 1819.39 mg/kg for MMT/BC). In order to determine the atrazine sorption equilibrium, the next experiment time was determined as 72 h.

The corresponding fitting parameters and the coefficient of determination (R^2) values are shown in **Table 2**. Compared with the first-order and second-order sorption kinetic models, the Elovich models fit the experimental data better with $R^2 >$ 0.97 (0.974 for BC and 0.988 for MMT/BC); the second was second-order (0.909 for BC and 0.914 for MMT/BC), and the worst was first-order (0.836 for BC and 0.848 for MMT/BC). The results revealed that atrazine sorption to the BC and MMT/BC was controlled by multiple mechanisms (Yao et al., 2014).

Sorption Isotherms of Atrazine on Biochar

Sorption isotherms of atrazine on BC and MMT/BC are shown in **Figures 5C,D**. All three isotherm models fit the data well, and the parameters are shown in **Table 2**. The dual-mode model has better fitting performance than Freundlich and Langmuir, with R^2 of 0.992 for BC and 0.996 for MMT/BC. The results revealed that sorption of atrazine on BC and MMT/BC was mainly partition and surface adsorption (Tang et al., 2015). Compared to BC, the Q value of atrazine on MMT/BC was increased from 592.99 to 1920.18 mg/kg. Therefore, the maximum capacity of MMT/BC on atrazine was about 3.2 times greater than that of BC. Hence, the modification method of MMT in this study could effectively improve the performance of biochar.

Effects of Solution pH

The effects of pH on atrazine sorption by MMT/BC are presented in **Supplementary Figure S4**. The sorption capacity was strongly affected by the initial pH of the aqueous solution. In brief, the uptake of atrazine decreased from 2,337.98 (pH = 2) to 1,292.89 mg/kg (pH = 9), with the increase of the pH value. It has been reported that the solution pH may change the degree of ionization of pesticide molecule, surface charge, and extent of dissociation of functional groups on the active sites of the biochar (Nandi et al., 2009). Atrazine is a weak alkaline pesticide with pKa value of 1.7, mainly exists as neutral molecule in the environment of pH 5–9, and promotes the formation of triazine cation at very low pH (Zheng et al., 2010). The MMT/BC surface was negatively charged at pH > 2.7, and it was combined with the triazine cations of atrazine by electrostatic interaction. Moreover, triazine cation could be exchanged with interlayer hydrated cations (Na^+ and Ca^{2+}) to enter the interlayer space of MMT (Premarathna et al., 2019). Therefore, the sorption capacity of MMT/BC to atrazine under low pH was high. At high pH, sorption was barely influenced by pH; this was similar to the result of Tan et al. (2016). Although, physisorption dominated, chemical sorption by chemical bonding and the increase of effective binding area caused by MMT deposition on the surface of biochar also promoted the sorption (Premarathna et al., 2019).

Sorption Mechanism Analysis

For both the BC and MMT/BC, the aromatic carbon on the surface of biochar can used as both an electron acceptor and an electron donor. The heterocyclic ring in atrazine is a π electron donor, so atrazine can interact with biochar through π-π electron donor–acceptor interactions (Sun et al., 2010; Zhao et al., 2013). Atrazine could also be used as hydrogen donors and acceptors to form hydrogen bonds with H, N, or O on the surface of biochar, further enhancing the sorption affinity of biochar. For both BC and MMT/BC, the sorption of atrazine is mainly chemical interactions, such as π–π interaction, hydrogen bonding, ion exchange, and electrostatic interactions. Due to the porosity of biochar, physical sorption may also be carried out *via* pore filling mechanism. In addition, the high surface activity and interlayer spaces of MMT improved the sorption

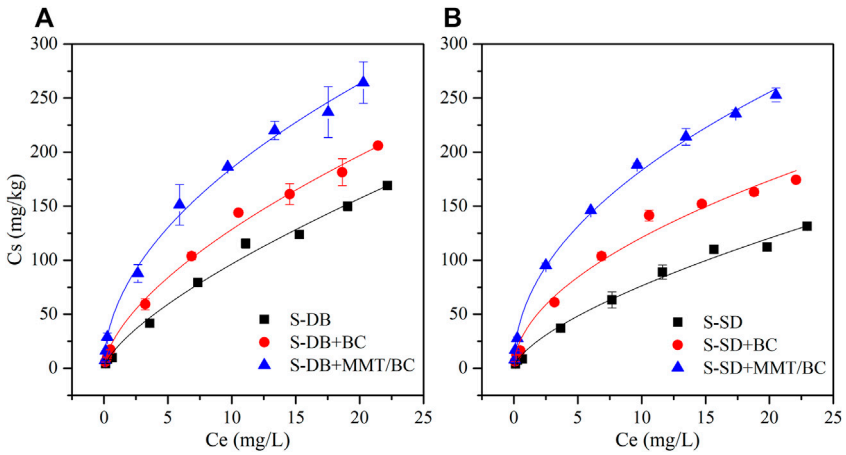

FIGURE 6 | Sorption isotherms of atrazine onto soil, BC-soil mixtures, and MMT/BC-soil mixtures [**(A)**: S-DB; **(B)**: S-SD). Isotherm data were fitted to Freundlich model.

TABLE 3 | Freundlich model of sorption isotherms of atrazine on soils and biochar–soil mixtures.

	Freundlich			K_d (L/kg)[a]		
	K_f (mg/kg)/(mg/L)^{nb}	n[c]	R^2	C_e = 0.05	C_e = 0.5	C_e = 5
S-DB	19.01 ± 2.31	0.70 ± 0.043	0.992	46.70	23.40	11.73
S-DB + BC	31.08 ± 2.62	0.62 ± 0.030	0.990	97.02	40.45	16.86
S-DB + MMT/BC	57.35 ± 3.75	0.51 ± 0.025	0.995	248.91	80.54	26.06
S-SD	16.71 ± 2.05	0.66 ± 0.043	0.991	46.27	21.15	9.67
S-SD + BC	36.32 ± 4.46	0.52 ± 0.045	0.983	152.98	50.66	16.77
S-SD + MMT/BC	60.48 ± 3.11	0.48 ± 0.019	0.996	287.18	86.73	26.19

[a]*Kd (L/kg) is the sorption coefficient estimated from the Freundlich sorption isotherms using Kd = Cs/Ce at Ce = 0.05, 0.5, and 5 mg/L.*
[b]*K_f [(mg/kg)/(mg/L)^n] is the Freundlich affinities related to sorption capacity.*
[c]*n is the isotherm nonlinearity factors of sorption.*

capacity of MMT/BC for atrazine through both surface sorption and intercalation interactions. So, MMT/BC was an effective adsorbent to remove atrazine from aqueous solution compared with BC.

Sorption of Atrazine on Soils and Biochar–Soil Mixtures

The sorption isotherms (**Figure 6**) were fitted using the Freundlich model (**Eq. 4**), and the parameters of the atrazine in two agricultural soils and biochar–soil mixtures are shown in **Table 3**. The Freundlich model can well describe the sorption data of atrazine ($R^2 > 0.98$). It was well documented that organic matter affects the sorption potential of soils, and higher organic matter content leads to more contaminants sorption (Fenoll et al., 2011). The organic matter contents of S-DB and S-SD were 41.0 and 29.2 g/kg, respectively, so the K_f of S-DB [19.01 (mg/kg)/(mg/L)^n] was higher than that of S-SD [16.71 (mg/kg)/(mg/L)^n]. The addition of biochar increased the sorption affinity of atrazine in soil, and the effect of MMT/BC is more obvious. For S-DB, the addition of BC increased K_f to 31.08 (mg/kg)/(mg/L)^n and the addition of MMT/BC increased to 57.35 (mg/kg)/(mg/L)^n; for S-SD, the addition of BC increased K_f to 36.32 (mg/kg)/(mg/L)^n and the addition of MMT/BC increased to 60.48 (mg/kg)/(mg/L)^n. The n values for biochar-amended soils were less than that of unamended soils, which indicated that the degree of isotherm non-linearity increased after biochar amendment, especially MMT/BC. Due to the non-linearity of the isotherms, the distribution coefficients (K_d) of three equilibrium concentrations (C_e = 0.05, 0.5, and 5 mg/L) were calculated (**Table 3**). Similar to K_f, the K_d of the soil was also increased with biochar amendment, and the K_d values of all the soils and biochar–soil mixtures decreased with increasing atrazine concentration. Previous studies have shown that water-soluble organic matters could be sorbed by biochar and compete with the added organic matter for limited sorption site or pores of biochar, thus reducing the sorption capacity of biochar (Cornelissen et al., 2005; Koelmans et al., 2009). However, organic substances may diffuse through the humic layer into biochar micropores overtime (Pignatello et al., 2006). Obviously, in the current research, atrazine may reach the micropores of biochar through the humic layer, thus improving the sorption capacity of atrazine.

Degradation of Atrazine in Soil and Biochar–Soil Mixtures

The degradation parameters of atrazine in soils and biochar–soil mixtures for 120 days under sterilized and non-sterilized conditions are shown in **Table 4**. The degradation curves of atrazine in non-

TABLE 4 | Degradation of atrazine in soils and biochar–soil mixtures during 120 days of incubation.

Soils		k (day^{-1})	R^2	$t_{1/2}$ (days)	Total removal (%)
S-DB	Unsterilized	0.024 ± 0.0022	0.9643	29.1	89.39[a]
	Sterilized	0.0020 ± 0.00046	0.6272	341.5	26.49[e]
S-DB + 2% MMT/BC	Unsterilized	0.0071 ± 0.0022	0.3765	97.8	60.54[c]
	Sterilized	0.0058 ± 0.0013	0.7554	119.7	58.05[c]
S-SD	Unsterilized	0.017 ± 0.0014	0.9650	40.5	81.69[b]
	Sterilized	0.0013 ± 0.00043	0.4087	521.2	21.10[f]
S-SD + 2% MMT/BC	Unsterilized	0.0055 ± 0.0019	0.4167	126.7	59.13[c]
	Sterilized	0.0042 ± 0.00035	0.9360	166.6	40.00[d]

Values represent the mean ± SD (n = 3). Values with the different letter (a–f) in the column indicate a statistically significant difference ($p < 0.05$).

sterilized S-DB and S-SD were fitted well with the first-order reaction kinetics model ($R^2 > 0.96$), and the half-lives were 29.1 and 40.5 days, respectively. The degradation of atrazine in S-DB was faster than that in S-SD; the main reason could be the high content of organic matter in S-DB, which can serve as an energy source to stimulate microbial activities and accelerate the degradation of pesticides (Gavrilescu, 2005; Briceño et al., 2007). However, in sterilized soils, the half-lives increased to 341.5 and 521.2 days, indicating that soil microbial was the main reason for atrazine degradation. After MMT/BC addition, the half-lives of atrazine in the non-sterilized soils increased (from 29.1 to 97.8 days for S-DB and 40.5 days to 126.7 for S-SD) and the degradation amount decreased (from 89.39% to 60.54% for S-DB and 81.69%–59.13% for S-SD). Previous studies have shown that biochar application in soil could reduce the biodegradation of pesticides (such as atrazine, acetochlor, diuron, and acetamiprid) by enhancing its sorption to the soil (Yang et al., 2006; Loganathan et al., 2009; Yu et al., 2011; Li et al., 2018) because the sorbed pesticides can only be biodegraded after being desorbed by the soil and diffused into the soil solution (Yu et al., 2011). The strong sorption of atrazine by MMT/BC made atrazine difficult to desorb, and atrazine was not easy to be degraded by microorganism; therefore, the degradation of atrazine was delayed. For sterilization treatment, the addition of MMT/BC accelerated the degradation of atrazine, indicating that biochar promoted the chemical degradation. It has been proved that biochar can also affect the chemical degradation of pesticides; Zhang et al. (2018) reported that the active groups on the biochar mineral surface played an important role in the chemical degradation of thiacloprid in biochar–soil mixtures. However, the mechanism of atrazine chemical degradation by MMT/BC remains to be further studied.

CONCLUSION

In this study, a montmorillonite–biochar composite (MMT/BC) was prepared *via* slow pyrolysis of MMT pretreated peanut shells for atrazine remediation. Structure and morphology analysis of raw biochar (BC) and MMT/BC showed that MMT particles have been successfully coated on the surface of biochar. However, excessive MMT particles will reduce the sorption capacity of biochar; 25% MMT was the best ratio of composite materials. MMT/BC was also affected by pyrolysis temperature; the higher the temperature (600°C), the better the sorption effect. Sorption experiments indicated that MMT/BC has higher removal capacity of atrazine than that of BC. The sorption of atrazine to MMT/BC was depended on pore-filling, π–π interaction, hydrogen bonding, ion exchange, and electrostatic interactions, and the high surface activity and interlayer spaces of MMT also improved the sorption capacity of MMT/BC through both surface sorption and intercalation interactions. In addition, the amendment of MMT/BC in soil improved the sorption capacity and delayed the degradation of atrazine. The results showed that MMT-modified biochar was a promising soil amendment to control atrazine contamination. According to the sorption and degradation mechanism of biochar and soil properties, it provided a basis for the selection of an effective biochar sorbent.

DATA AVAILABILITY STATEMENT

The original contributions presented in the study are included in the article/**Supplementary Material**, further inquiries can be directed to the corresponding author.

AUTHOR CONTRIBUTIONS

PW: conceptualization, methodology, data curation, formal analysis, investigation, validation, and writing—original draft. MS, LW, SY, LM, LZZ, LZ, YZ, and HJ: supervision. YZ: conceptualization, resources, supervision, and project administration. XL: supervision. resources, project administration, writing—review and editing, and funding acquisition.

FUNDING

This work was supported by the National Natural Science Foundation of China (32102269 and 31861133021).

SUPPLEMENTARY MATERIAL

The Supplementary Material for this article can be found online at: https://www.frontiersin.org/articles/10.3389/fenvs.2022.888252/full#supplementary-material

REFERENCES

Akhavan, O. (2010). Graphene Nanomesh by ZnO Nanorod Photocatalysts. *ACS nano* 4, 4174–4180. doi:10.1021/nn1007429

Briceño, G., Palma, G., and Durán, N. (2007). Influence of Organic Amendment on the Biodegradation and Movement of Pesticides. *Crit. Rev. Environ. Sci. Technol.* 37, 233–271. doi:10.1080/10643380600987406

Chen, B., Zhou, D., and Zhu, L. (2008). Transitional Adsorption and Partition of Nonpolar and Polar Aromatic Contaminants by Biochars of pine needles with Different Pyrolytic Temperatures. *Environ. Sci. Technol.* 42, 5137–5143. doi:10.1021/es8002684

Chen, C., Yang, S., Guo, Y., Sun, C., Gu, C., and Xu, B. (2009). Photolytic Destruction of Endocrine Disruptor Atrazine in Aqueous Solution under UV Irradiation: Products and Pathways. *J. Hazard. Mater.* 172, 675–684. doi:10.1016/j.jhazmat.2009.07.050

Chen, L., Chen, X. L., Zhou, C. H., Yang, H. M., Ji, S. F., Tong, D. S., et al. (2017). Environmental-friendly Montmorillonite-Biochar Composites: Facile Production and Tunable Adsorption-Release of Ammonium and Phosphate. *J. Clean. Prod.* 156, 648–659. doi:10.1016/j.jclepro.2017.04.050

Cornelissen, G., Gustafsson, Ö., Bucheli, T. D., Jonker, M. T. O., Koelmans, A. A., and Van Noort, P. C. M. (2005). Extensive Sorption of Organic Compounds to Black Carbon, Coal, and Kerogen in Sediments and Soils: Mechanisms and Consequences for Distribution, Bioaccumulation, and Biodegradation. *Environ. Sci. Technol.* 39, 6881–6895. doi:10.1021/es050191b

Fang, W., Wang, Q., Han, D., Liu, P., Huang, B., Yan, D., et al. (2016). The Effects and Mode of Action of Biochar on the Degradation of Methyl Isothiocyanate in Soil. *Sci. Total Environ.* 565, 339–345. doi:10.1016/j.scitotenv.2016.04.166

Fenoll, J., Ruiz, E., Flores, P., Hellín, P., and Navarro, S. (2011). Reduction of the Movement and Persistence of Pesticides in Soil through Common Agronomic Practices. *Chemosphere* 85, 1375–1382. doi:10.1016/j.chemosphere.2011.07.063

Ferrari, A. C., and Robertson, J. (2000). Interpretation of Raman Spectra of Disordered and Amorphous Carbon. *Phys. Rev. B* 61, 14095–14107. doi:10.1103/PhysRevB.61.14095

Fosso-Kankeu, E., Waanders, F. B., and Steyn, F. W. (2015). "The Preparation and Characterization of clay-biochar Composites for the Removal of Metal Pollutants," in 7th International Conference on latest Trends in Engineering and Technology (ICLTET'2015), Irene Pretoria South Africa, 54–57.

Gao, X., Wu, L., Li, Z., Xu, Q., Tian, W., and Wang, R. (2018). Preparation and Characterization of High Surface Area Activated Carbon from pine wood Sawdust by Fast Activation with H3PO4 in a Spouted Bed. *J. Mater. Cycles Waste Manag.* 20, 925–936. doi:10.1007/s10163-017-0653-x

Gavrilescu, M. (2005). Fate of Pesticides in the Environment and its Bioremediation. *Eng. Life Sci.* 5, 497–526. doi:10.1002/elsc.200520098

Hayes, T., Haston, K., Tsui, M., Hoang, A., Haeffele, C., and Vonk, A. (2003). Atrazine-induced Hermaphroditism at 0.1 Ppb in American Leopard Frogs (Rana pipiens): Laboratory and Field Evidence. *Environ. Health Perspect.* 111, 568–575. doi:10.1289/ehp.5932

Inyang, M., Gao, B., Zimmerman, A., Zhang, M., and Chen, H. (2014). Synthesis, Characterization, and Dye Sorption Ability of Carbon Nanotube-Biochar Nanocomposites. *Chem. Eng. J.* 236, 39–46. doi:10.1016/j.cej.2013.09.074

Jablonowski, N. D., Hamacher, G., Martinazzo, R., Langen, U., Köppchen, S., Hofmann, D., et al. (2010). Metabolism and Persistence of Atrazine in Several Field Soils with Different Atrazine Application Histories. *J. Agric. Food Chem.* 58, 12869–12877. doi:10.1021/jf103577j

Jansen, R. J. J., and Van Bekkum, H. (1995). XPS of Nitrogen-Containing Functional Groups on Activated Carbon. *Carbon* 33, 1021–1027. doi:10.1016/0008-6223(95)00030-H

Jin, J., Kang, M., Sun, K., Pan, Z., Wu, F., and Xing, B. (2016). Properties of Biochar-Amended Soils and Their Sorption of Imidacloprid, Isoproturon, and Atrazine. *Sci. Total Environ.* 550, 504–513. doi:10.1016/j.scitotenv.2016.01.117

Jing, X.-R., Wang, Y.-Y., Liu, W.-J., Wang, Y.-K., and Jiang, H. (2014). Enhanced Adsorption Performance of Tetracycline in Aqueous Solutions by Methanol-Modified Biochar. *Chem. Eng. J.* 248, 168–174. doi:10.1016/j.cej.2014.03.006

Keiluweit, M., Nico, P. S., Johnson, M. G., and Kleber, M. (2010). Dynamic Molecular Structure of Plant Biomass-Derived Black Carbon (Biochar). *Environ. Sci. Technol.* 44, 1247–1253. doi:10.1021/es9031419

Koelmans, A. A., Meulman, B., Meijer, T., and Jonker, M. T. O. (2009). Attenuation of Polychlorinated Biphenyl Sorption to Charcoal by Humic Acids. *Environ. Sci. Technol.* 43, 736–742. doi:10.1021/es802862b

Li, J., Li, S., Dong, H., Yang, S., Li, Y., and Zhong, J. (2015). Role of Alumina and Montmorillonite in Changing the Sorption of Herbicides to Biochars. *J. Agric. Food Chem.* 63, 5740–5746. doi:10.1021/acs.jafc.5b01654

Li, Y., Liu, X., Wu, X., Dong, F., Xu, J., Pan, X., et al. (2018). Effects of Biochars on the Fate of Acetochlor in Soil and on its Uptake in maize Seedling. *Environ. Pollut.* 241, 710–719. doi:10.1016/j.envpol.2018.05.079

Li, Y., Wang, Z., Xie, X., Zhu, J., Li, R., and Qin, T. (2017a). Removal of Norfloxacin from Aqueous Solution by clay-biochar Composite Prepared from Potato Stem and Natural Attapulgite. *Colloids Surf. A: Physicochemical Eng. Aspects* 514, 126–136. doi:10.1016/j.colsurfa.2016.11.064

Li, Y., Zhu, Y., Liu, X., Wu, X., Dong, F., Xu, J., et al. (2017b). Bioavailability Assessment of Thiacloprid in Soil as Affected by Biochar. *Chemosphere* 171, 185–191. doi:10.1016/j.chemosphere.2016.12.071

Liang, G., Wang, Z., Yang, X., Qin, T., Xie, X., Zhao, J., et al. (2019). Efficient Removal of Oxytetracycline from Aqueous Solution Using Magnetic Montmorillonite-Biochar Composite Prepared by One Step Pyrolysis. *Sci. Total Environ.* 695, 133800. doi:10.1016/j.scitotenv.2019.133800

Liu, N., Charrua, A. B., Weng, C.-H., Yuan, X., and Ding, F. (2015). Characterization of Biochars Derived from Agriculture Wastes and Their Adsorptive Removal of Atrazine from Aqueous Solution: A Comparative Study. *Bioresour. Technology* 198, 55–62. doi:10.1016/j.biortech.2015.08.129

Loganathan, V. A., Feng, Y., Sheng, G. D., and Clement, T. P. (2009). Crop-Residue-Derived Char Influences Sorption, Desorption and Bioavailability of Atrazine in Soils. *Soil Sci. Soc. Am. J.* 73, 967–974. doi:10.2136/sssaj2008.0208

Lyu, H., Gao, B., He, F., Ding, C., Tang, J., and Crittenden, J. C. (2017a). Ball-milled Carbon Nanomaterials for Energy and Environmental Applications. *ACS Sustainable Chem. Eng.* 5, 9568–9585. doi:10.1021/acssuschemeng.7b02170

Lyu, H., Tang, J., Huang, Y., Gai, L., Zeng, E. Y., Liber, K., et al. (2017b). Removal of Hexavalent Chromium from Aqueous Solutions by a Novel Biochar Supported Nanoscale Iron Sulfide Composite. *Chem. Eng. J.* 322, 516–524. doi:10.1016/j.cej.2017.04.058

Mueller, A., Schwab, M. G., Encinas, N., Vollmer, D., Sachdev, H., and Müllen, K. (2015). Generation of Nitrile Groups on Graphites in a Nitrogen RF-Plasma Discharge. *Carbon* 84, 426–433. doi:10.1016/j.carbon.2014.11.054

Nandi, B. K., Goswami, A., and Purkait, M. K. (2009). Adsorption Characteristics of Brilliant green Dye on Kaolin. *J. Hazard. Mater.* 161, 387–395. doi:10.1016/j.jhazmat.2008.03.110

Novak, J. M., Lima, I., Xing, B. S., Gaskin, J. W., Steiner, C., Das, K. C., et al. (2009). Characterization of Designer Biochar Produced at Different Temperatures and Their Effects on a Loamy Sand. *Ann. Environ. Sci.* 3, 195–206.

Pignatello, J. J., Kwon, S., and Lu, Y. (2006). Effect of Natural Organic Substances on the Surface and Adsorptive Properties of Environmental Black Carbon (Char): Attenuation of Surface Activity by Humic and Fulvic Acids. *Environ. Sci. Technol.* 40, 7757–7763. doi:10.1021/es061307m

Premarathna, K. S. D., Rajapaksha, A. U., Adassoriya, N., Sarkar, B., Sirimuthu, N. M. S., Cooray, A., et al. (2019). Clay-biochar Composites for Sorptive Removal of Tetracycline Antibiotic in Aqueous media. *J. Environ. Manag.* 238, 315–322. doi:10.1016/j.jenvman.2019.02.069

Qu, M., Li, H., Li, N., Liu, G., Zhao, J., Hua, Y., et al. (2017). Distribution of Atrazine and its Phytoremediation by Submerged Macrophytes in lake Sediments. *Chemosphere* 168, 1515–1522. doi:10.1016/j.chemosphere.2016.11.164

Singh, R. P., Ahsan, M., Mishra, D., Pandey, V., AnupamaYadav, A., Yadav, A., et al. (2022). Ameliorative Effects of Biochar on Persistency, Dissipation, and Toxicity of Atrazine in Three Contrasting Soils. *J. Environ. Manage.* 303, 114146. doi:10.1016/j.jenvman.2021.114146

Solomon, K. R., Baker, D. B., Richards, R. P., Dixon, K. R., Klaine, S. J., La Point, T. W., et al. (1996). Ecological Risk Assessment of Atrazine in North American Surface Waters. *Environ. Toxicol. Chem.* 15, 31–76. doi:10.1002/etc.205010.1002/etc.5620150105

Song, J., Zhang, S., Li, G., Du, Q., and Yang, F. (2020). Preparation of Montmorillonite Modified Biochar with Various Temperatures and Their Mechanism for Zn Ion Removal. *J. Hazard. Mater.* 391, 121692. doi:10.1016/j.jhazmat.2019.121692

Sun, K., Gao, B., Zhang, Z., Zhang, G., Zhao, Y., and Xing, B. (2010). Sorption of Atrazine and Phenanthrene by Organic Matter Fractions in Soil and Sediment. *Environ. Pollut.* 158, 3520–3526. doi:10.1016/j.envpol.2010.08.022

Suo, F., You, X., Ma, Y., and Li, Y. (2019). Rapid Removal of Triazine Pesticides by P Doped Biochar and the Adsorption Mechanism. *Chemosphere* 235, 918–925. doi:10.1016/j.chemosphere.2019.06.158

Swan, S. H., Kruse, R. L., Liu, F., Barr, D. B., Drobnis, E. Z., Redmon, J. B., et al. (2003). Study Future Families Res, GSemen Quality in Relation to Biomarkers of Pesticide Exposure. *Environ. Health Perspect.* 111, 1478–1484. doi:10.1289/ehp.6417

Tan, G., Sun, W., Xu, Y., Wang, H., and Xu, N. (2016). Sorption of Mercury (II) and Atrazine by Biochar, Modified Biochars and Biochar Based Activated Carbon in Aqueous Solution. *Bioresour. Technol.* 211, 727–735. doi:10.1016/j.biortech.2016.03.147

Tang, J., Lv, H., Gong, Y., and Huang, Y. (2015). Preparation and Characterization of a Novel Graphene/biochar Composite for Aqueous Phenanthrene and Mercury Removal. *Bioresour. Technology* 196, 355–363. doi:10.1016/j.biortech.2015.07.047

Tappe, W., Groeneweg, J., and Jantsch, B. (2002). Diffuse Atrazine Pollution in German Aquifers. *Biodegradation* 13, 3–10. doi:10.1023/a:1016325527709

Tyagi, B., Chudasama, C. D., and Jasra, R. V. (2006). Determination of Structural Modification in Acid Activated Montmorillonite clay by FT-IR Spectroscopy. *Spectrochimica Acta A: Mol. Biomol. Spectrosc.* 64, 273–278. doi:10.1016/j.saa.2005.07.018

Uchimiya, M., Wartelle, L. H., Lima, I. M., and Klasson, K. T. (2010). Sorption of Deisopropylatrazine on Broiler Litter Biochars. *J. Agric. Food Chem.* 58, 12350–12356. doi:10.1021/jf102152q

Wang, P., Liu, X., Yu, B., Wu, X., Xu, J., Dong, F., et al. (2020). Characterization of Peanut-Shell Biochar and the Mechanisms Underlying its Sorption for Atrazine and Nicosulfuron in Aqueous Solution. *Sci. Total Environ.* 702, 134767. doi:10.1016/j.scitotenv.2019.134767

Wu, C., Liu, X., Wu, X., Dong, F., Xu, J., and Zheng, Y. (2019). Sorption, Degradation and Bioavailability of Oxyfluorfen in Biochar-Amended Soils. *Sci. Total Environ.* 658, 87–94. doi:10.1016/j.scitotenv.2018.12.059

Yang, X.-B., Ying, G.-G., Peng, P.-A., Wang, L., Zhao, J.-L., Zhang, L.-J., et al. (2010). Influence of Biochars on Plant Uptake and Dissipation of Two Pesticides in an Agricultural Soil. *J. Agric. Food Chem.* 58, 7915–7921. doi:10.1021/jf1011352

Yang, Y., Sheng, G., and Huang, M. (2006). Bioavailability of Diuron in Soil Containing Wheat-Straw-Derived Char. *Sci. Total Environ.* 354, 170–178. doi:10.1016/j.scitotenv.2005.01.026

Yao, Y., Gao, B., Fang, J., Zhang, M., Chen, H., Zhou, Y., et al. (2014). Characterization and Environmental Applications of clay-biochar Composites. *Chem. Eng. J.* 242, 136–143. doi:10.1016/j.cej.2013.12.062

Yu, X.-Y., Mu, C.-L., Gu, C., Liu, C., and Liu, X.-J. (2011). Impact of Woodchip Biochar Amendment on the Sorption and Dissipation of Pesticide Acetamiprid in Agricultural Soils. *Chemosphere* 85, 1284–1289. doi:10.1016/j.chemosphere.2011.07.031

Zhang, G., Zhang, Q., Sun, K., Liu, X., Zheng, W., and Zhao, Y. (2011). Sorption of Simazine to Corn Straw Biochars Prepared at Different Pyrolytic Temperatures. *Environ. Pollut.* 159, 2594–2601. doi:10.1016/j.envpol.2011.06.012

Zhang, M., and Gao, B. (2013). Removal of Arsenic, Methylene Blue, and Phosphate by biochar/AlOOH Nanocomposite. *Chem. Eng. J.* 226, 286–292. doi:10.1016/j.cej.2013.04.077

Zhang, P., Sun, H., Min, L., and Ren, C. (2018). Biochars Change the Sorption and Degradation of Thiacloprid in Soil: Insights into Chemical and Biological Mechanisms. *Environ. Pollut.* 236, 158–167. doi:10.1016/j.envpol.2018.01.030

Zhao, X., Ouyang, W., Hao, F., Lin, C., Wang, F., Han, S., et al. (2013). Properties Comparison of Biochars from Corn Straw with Different Pretreatment and Sorption Behaviour of Atrazine. *Bioresour. Technology* 147, 338–344. doi:10.1016/j.biortech.2013.08.042

Zheng, H., Bao, J., Huang, Y., Xiang, L., Faheem, B., Ren, B., et al. (2019). Efficient Degradation of Atrazine with Porous Sulfurized Fe2O3 as Catalyst for Peroxymonosulfate Activation. *Appl. Catal. B: Environ.* 259, 118056. doi:10.1016/j.apcatb.2019.118056

Zheng, W., Guo, M., Chow, T., Bennett, D. N., and Rajagopalan, N. (2010). Sorption Properties of Greenwaste Biochar for Two Triazine Pesticides. *J. Hazard. Mater.* 181, 121–126. doi:10.1016/j.jhazmat.2010.04.103

Zhou, J.-H., Sui, Z.-J., Zhu, J., Li, P., Chen, D., Dai, Y.-C., et al. (2007). Characterization of Surface Oxygen Complexes on Carbon Nanofibers by TPD, XPS and FT-IR. *Carbon* 45, 785–796. doi:10.1016/j.carbon.2006.11.019

Zhou, L., Chen, H., Jiang, X., Lu, F., Zhou, Y., Yin, W., et al. (2009). Modification of Montmorillonite Surfaces Using a Novel Class of Cationic Gemini Surfactants. *J. Colloid Interf. Sci.* 332, 16–21. doi:10.1016/j.jcis.2008.12.051

Zhu, L., Yang, H., Zhao, Y., Kang, K., Liu, Y., He, P., et al. (2019). Biochar Combined with Montmorillonite Amendments Increase Bioavailable Organic Nitrogen and Reduce Nitrogen Loss during Composting. *Bioresour. Technol.* 294, 122224. doi:10.1016/j.biortech.2019.122224

Conflict of Interest: The authors declare that the research was conducted in the absence of any commercial or financial relationships that could be construed as a potential conflict of interest.

Publisher's Note: All claims expressed in this article are solely those of the authors and do not necessarily represent those of their affiliated organizations, or those of the publisher, the editors, and the reviewers. Any product that may be evaluated in this article, or claim that may be made by its manufacturer, is not guaranteed or endorsed by the publisher.